THESIS FOR THE DEGREE OF LICENTIATE ENGINEERING

Surface Characterization of Soft Magnetic Composite Powder and Compacts

Christos Oikonomou

Department of Materials and Manufacturing Technology
CHALMERS UNIVERSITY OF TECHNOLOGY
Gothenburg, Sweden 2014

Surface Characterization of Soft Magnetic Composite Powder and Compacts

CHRISTOS OIKONOMOU

Department of Materials and Manufacturing Technology
Chalmers University of Technology
SE-412 96 Gothenburg
Sweden
Telephone: ++46(0)31-772 1000

"I thank y'all for letting me be here with you.
Whether I know what to say about it or not, it means a lot to me,
and I thank you, okay?"

-SRV

Surface Characterization of Soft Magnetic Composite Powder and Compacts

Christos Oikonomou

Department of Materials and Manufacturing Technology
Chalmers University of Technology

Abstract

Soft Magnetic Composite (SMC) components produced based on traditional Powder Metallurgical (PM) techniques, are strong candidate materials for electromagnetic applications. Their advantages are based on profitable and energy efficient production methods, shape complexity realization and uniquely uniform and isotropic 3D magnetic properties. SMC powder grades consist of individually encapsulated iron powder particles with an ultra-fine, electrically insulating surface coating. Component manufacturing procedure involves compaction of the admixed SMC base powder with a lubricant to a final shape, as well as a subsequent heat-treatment that aims on the relaxation of stresses induced during the compaction. The concept of SMC is based on taking advantage of the insulating properties of the surface coating and creating a laminated stack in a powder form. In this manner, products with comparable or superior magnetic performances can be produced as opposed to the more traditional laminated steels and ferrites, due to the higher reduction of eddy currents especially at high frequency applications.

The insulating coating constitutes the paramount feature of the SMC technology. Its morphology, thickness, cohesion to the powder particles surface and durability during processing, are critical aspects to the properties of a finished component. Hence, a methodology based on analytical techniques was developed and implemented on commercially available SMC base powder and finished components, in order to address these matters for such insulating coatings on a micro-level. Standard methods previously used for the powder surface characterization have been significantly modified due to the non-conductive nature of the surface coating. A theoretical model for thickness determination of the surface layer for powders, based on X-ray photoelectron spectroscopy (XPS) depth profiling, was further developed and experimentally evaluated. The theoretical results showed only minor deviations of the order of 3% with the experimental values. The novelty of the latter lies in its ability to take into account the artifacts imposed to an analysis due to the geometries of the sample and of the current experimental arrangement.

The surface analysis of the SMC base powder revealed the presence of a uniform, inorganic, iron phosphate based coating with good overall coverage and coherence to the core. Its chemical depth profile was evaluated and its thickness was determined by implementing the theoretical model. Additionally, the thermal stability of the insulating coating of finished SMC components was investigated under different temperature regimes. The implementation of the previously developed methodology highlighted the difference of the heat-treatment effect on the interior and exterior regions of the components in terms of surface chemistry. In this context, increased oxidation was observed in the area close to the surface of the parts, as opposed to the center, while the analysis also showed that incomplete de-lubrication is taking place at temperatures below 500°C.

V

Preface

This licentiate thesis is based on the work performed at the department of Materials and Manufacturing Technology at Chalmers University of Technology between January 2011 and December 2013. The project has been carried out under the supervision of Associate Professor Eduard Hryha and Professor Lars Nyborg.

This thesis consists of an introductory part followed by the appended technical papers:

Paper I: Evaluation of the thickness and roughness of homogeneous surface layers on spherical and irregular powder particles
C. Oikonomou, D. Nikas, E. Hryha, L. Nyborg
Early View (Online Version of Record published before inclusion in an issue)

Paper II: Development of methodology for surface analysis of soft magnetic composite powders
C. Oikonomou, E. Hryha, L. Nyborg
Surface and Interface Analysis
Volume 44, Issue 8, pages 1166–1170, August 2012

Paper III: Effect of Heat Treatment in Air on Surface Composition of Soft Magnetic Composite Components
C. Oikonomou, R. Oro, E. Hryha, L. Nyborg
Submitted for publication in Materials Science and Engineering: B

The author performed the experimental part of the thesis except the FIB measurements in Paper I and XRD measurements in Paper III that were carried out by Dr. Yiming Yao and Dr. Raquel De Oro Calderón respectively. The source code for the computer software that was developed for the needs of the theoretical model presented in this thesis was written by Yaroslav Kish. The author wrote the first draft versions of the papers and finalized them in close collaboration with Professor Lars Nyborg and Associate Professor Eduard Hryha.

Table of contents

x

1. Introduction

In this section, a brief description of Soft Magnetic Composite materials is given along with the thesis scope and goals for contributing to this field.

1.1. Background

Energy efficiency strategies have drawn much attention in the last decades, constituting a major part of the whole sustainable energy development effort. Nowadays, new policies for energy preservation are being introduced globally along with new legislations that target to the stabilization and reduction of the total CO_2 emissions in energy production, residential and commercial consumption, transportation and industry [1]. In this context, electromagnetic applications can prove to be beneficial if one takes into account the possibilities of their involvement in all of these fields. Power circuits, communication devices, microelectronics, automotive applications, household appliances and many more categories of contemporary utilities, all make use of the electromagnetic effect for energy storage and conversion [2]. Related to these phenomena though are energy losses, namely core losses, due to inherent material properties that reduce the efficiency of the applications by dissipating energy in the form of heat. Hence, the need for new improved materials for such type of purposes is constant and basically driven by an outgrowing consumption demand.

Soft magnets comprise the other most important family of ferromagnetic materials, along with the hard magnets, which are defined by their ease to magnetize and demagnetize even when subjected to low external magnetic fields. They have been being widely used as core for inductors and transformers in both DC and AC applications [2, 3]. Typically, steel laminated structures and ferrites are preferred due to their higher electrical resistivity. This attribute is essential in reducing the core losses by preventing the circulation of the deleterious induced eddy currents, especially at higher frequencies. The growth though of fields such as information technology, high frequency applications and electric motors increase the demand for more sophisticated technologies, which in turn push towards size reduction and new complex designs that often test the limits of these more traditional solutions.

Promising alternatives to the latter are iron powdered cores, produced by compaction of individual electrically insulated powder particles under high pressures into compact solid forms. The idea behind this concept dates back to the 19th century, though the advance in materials science and production techniques have given it a significant boost in the last decades. These materials, often termed as Soft Magnetic Composites (SMC), are being manufactured today by conventional powder metallurgical techniques [4, 5]. Their advantages lie in their isotropic nature and high electrical resistivity, which open up new design possibilities for weight, energy losses and cost production reductions. Proper material selection and process treatment are hence important aspects that can further promote the flexibility of this technology in terms of applications. Therefore, the primary research volume

related to the improvement of SMC properties focuses on the development of more exotic and functional insulating materials, as well as various coating methods [6-8].

Thus, in order to promote this effort, the development of robust analysis methods can be proven crucial in delivering fundamental knowledge and tools in further understanding the materials under question.

1.2.Scope and goal of this study

The superior bulk electrical resistivity of SMC products, as compared to their laminated steel or ferrite counterparts, can be entirely attributed to the insulating material that encapsulates and separates each individual metal particle. Their electromagnetic performance is much dependent on the viability and behavior of this coating under different process treatments [9].

It is thus the scope of the present study to investigate the nature of such type of layers, both in as-received and processed forms. Their morphological, structural and chemical characterization as well as the assessment and improvement of their treatment are highly prioritized.

To achieve this, the goal was set initially to develop a methodology based on analytical techniques that would enable the evaluation of the homogeneity, chemical composition *vs* depth and thickness of the insulating coating. To that end, a theoretical model was additionally developed for surface products thickness determination using surface sensitive analytical technique and implemented to the material of interest. Finally, heat-treatment was selected for investigation as the most important process parameter influencing the state of the insulating coating, and hence the performance of the final SMC product. The effect of the heat-treatment parameters on the quality of the coating was assessed by means of the methodology developed.

2. Soft Magnetic Materials

In this section of the thesis, a brief introduction to the soft magnetic material is given that includes their classification based on their composition, properties and applications.

2.1. Overview

Both ferro- and ferrimagnetic materials have been generally divided into two large families, namely soft and hard magnets, based on their ease to magnetize and demagnetize under an applied field [10]. Their differences can be better illustrated by examining their hysteresis loops when subjected to a magnetization cycle under an externally applied magnetic field, as shown in Figure 1. In the case of a soft magnet (Fig. 16a), saturation is easily achieved even under fields of low strength which is not the case for a hard magnet (Fig. 16b).
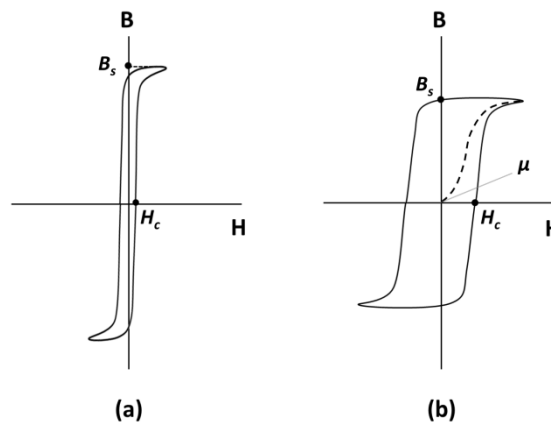
Figure 1: Hysteresis loops for (a) soft and (b) hard magnetic material.

It can be observed that for a material to be soft magnetic, its hysteresis loop should be as thin and high as possible. This translates to a low value of the coercive force of the material (the amount of the reverse applied field H_c that is needed to decrease the induction to zero), high value for its magnetic permeability μ (a measure of its magnetic sensitivity defined as B/H), and high saturation induction value, B_s.

Since hard magnetic materials are difficult to demagnetize, the energy stored to them and expressed as an external magnetic field will last indefinitely (or until an external source causes them to demagnetize). For this reason, they are used in applications where permanent magnets are required such as magnetic recording, memory devices, speakers and sensors, among others.

On the other hand, the ability of the soft magnets to easily magnetize and demagnetize renders them ideal candidates for both AC and DC applications. Thus, they are widely used as cores in transformers and inductors order to enhance and/or channel the produced magnetic flux [2, 3, 10].

2.2. Core losses

The dissipation of energy in a magnetic core during its magnetization and demagnetization cycle is widely termed as core losses. While these are not of high importance for hard magnets, they are crucial in the efficiency of soft magnetic applications and can be controlled with proper material selection [3, 4, 10]. Core losses are generally divided into three categories, namely hysteresis losses (P_h), eddy current losses (P_e) and residual losses (P_r).

The hysteresis loses originate from the movement of the domain walls back and forth under a magnetization/demagnetization loop. The presence of impurities, precipitates, imperfections, grain boundaries and dislocations act as barriers towards this motion and increase those loses. These can be measured from the internal area of the hysteresis loop and exhibit a linear relationship with the frequency of the applied field.

The eddy current losses, alternatively named classical eddy current losses, are caused by the existence of stray electric currents that circulate into the bulk of the material. The subjection of a magnetic material to a fluctuating magnetic field induces swirling currents in rotating patterns that eventually dissipate energy in the form of heat. Classical eddy currents are considered macroscopic and become extremely importance in high frequency applications due to their squared relationship with the latter.

The residual losses, also called anomalous losses or excess eddy current losses, are dynamic losses related to the circulation of the eddy currents due to domain wall motion but on the microscale [11, 12]. These are also material dependent and escalate with increasing frequency, but their contribution is indirectly measured from the difference of theoretical and experimental results.

2.3. Materials and applications.

In industrial soft magnetic applications, the ferromagnetic elements Fe, Co and Ni along with soft ferrites (i.e. ceramic compounds based on iron oxides with the addition of Ni, Zn and/or Mn), are the most important families of materials. They exist in different alloyed compositions and produced under various fabrication techniques in order to achieve the best ratio of performance and cost for a specific application. For example, iron-cobalt alloys are known as the materials with the highest saturation flux values but also for being very expensive, as compared to pure iron or iron-phosphorus products which have good induction values and low cost. Iron-nickel alloys on the other hand have the highest permeabilities while the iron-silicon system is extensively used for its low coercive force. These materials are mainly being manufactured either in the form of laminates stacks or as powdered cores depending on the designed application. In the first case, metal strips produced by different forming processes are joined together, while in the second case insulated powder particles are used as base material in finished products via sintering operations or by using various types of binder substances. In addition to the previous, nowadays the development of iron based

magnetic materials in amorphous and nano-crystalline forms by liquid quenching techniques is favored due to their low coercive force and high resistivity. Soft magnetic materials, as described earlier, are used typically for core applications in transformers, inductors, actuators, chokes, filters, sensors, detectors and contractors among others, in order to enhance and/or channel the produced magnetic flux.

In Table 1 some of the most commonly used soft magnetic materials are mentioned along with representative production techniques and applications.

Alloys	Production Techniques	Properties	Applications	References
Pure Fe	powdered (SMC/sintered)	good saturation flux /low cost	filters/pure inductors /power transformers /sensors/actuators /electric motors	[2-4, 13-15]
Fe-P	powdered (sintered)	good saturation /good mechanical properties/low cost	pure inductors /power transformers /rotary actuators/sensors	[2, 4, 16, 17]
Fe-Si	laminated /thin tapes /powdered (sintered)	good electrical resistivity /stability with age /good mechanical properties/low cost	pure inductors /power transformers /relays/solenoids	[2-4, 14, 16, 17]
Fe-Ni	thin tapes /powdered (sintered)	high permeability /low flux density /high cost	pure inductors /power transformers /actuators/detectors /sensors/contractors	[2-4, 14, 16, 17]
Fe-Ni-Mo	powdered (sintered)	high permeability /stability with time and temperature /high cost	loading coils/filtering coils/switching power supplies	[2, 3, 14]
Fe-Co	laminated /powdered (sintered)	high saturation flux/high cost	actuators/ aerospace motors/ high performance transformers/filters	[2, 4, 14, 16]
Soft ferrites	laminated /powdered (sintered)	high resistivity /low saturation flux /low cost	power transformers/filter inductors/sensors	[2, 3, 14, 16]
Fe-B-Si Fe-Co-Si Fe-Cu-Si Fe-C-P-B-Si-Mo Fe-B-Si-Nb Fe-P-B-Si	laminated /powdered	high magnetic permeability /good saturation flux / high resistivity	high frequency aerospace transformers	[2, 3, 18, 19]

Table 1: General classification of soft magnetic materials based on their composition, production techniques, properties and applications.

3. Soft magnetic Composites

In this section of the thesis, the concept soft magnetic composite materials is presented along with information on their processing and treatments.

3.1. Overview

Development of soft magnetic products for electromagnetic applications produced by conventional powder metallurgical techniques is a continuous growing field [2, 4, 5, 11, 13-17, 20]. These can be generally divide into two families, the ones produced by sintering of the base powdered material into finalized components and the ones who do not need sintering but the bonding is facilitated by the presence of various types of binding materials. In the first family belong the iron based alloys described in the previous section which are targeted for DC applications of less than 50Hz, exhibiting high saturation flux and good mechanical properties [4, 17, 21]. The second family, which is known as Soft Magnetic Composites (SMC), considers powdered parts that consist of individually encapsulated pure iron powder particles with an electrically insulating coating, bonded together in three dimensional structures (Figure 2) [5, 15, 20].
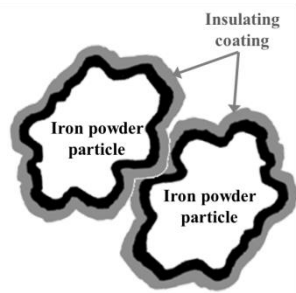
Figure 2: The SMC concept.

The advantages of using the SMC technology for electromagnetic applications are illustrated at Figure 3.
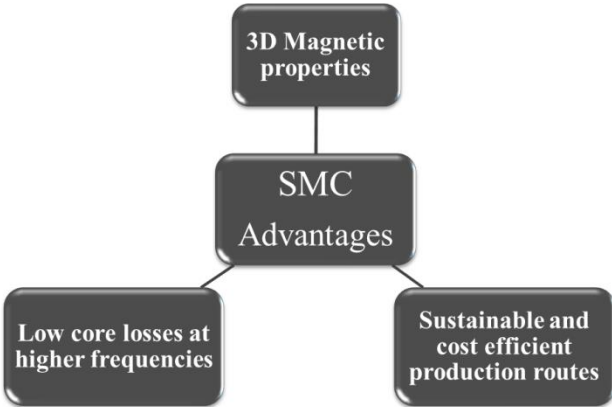
Figure 3: Advantages of the SMC technology.

The concept of the SMC aims in reducing the core losses in a part by introducing higher bulk resistivity through the increased insulating interfacial volume. This property can be tailored to the application of interest by varying the powder particle size and the thickness of the insulating coating. In this manner, the SMC technique offers a unique combination of magnetic saturation and resistivity levels, and consequently higher flexibility in terms of applications range as compared to the more traditionally used laminated steels and ferrites (Figure 4).
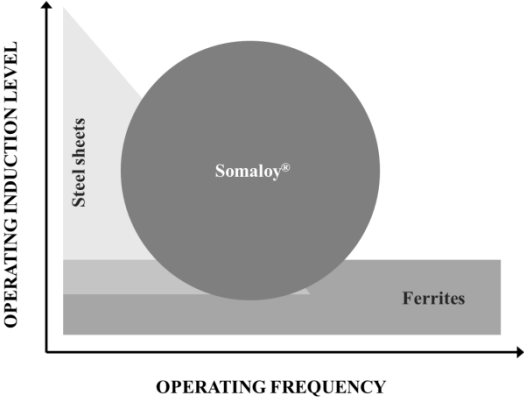
Figure 4: SMC positioning among laminated steels and ferrites in electromagnetic applications. Redrawn from [15]

Another advantage of the SMC technology lies in the fact that new design possibilities open up due to their isotropic nature. Unlike the laminate steels, SMC products can make use of their three dimensional (3D) flux capabilities and innovative and more sophisticated applications of higher complexity can now be realized, that lead to reduced size and copper winding necessary [13].

Moreover, the SMC products prove to be an appealing option for electromagnetic applications due to their cost low production cost. Taking advantage of the well-established manufacturing techniques offered by Powder Metallurgy (PM) industry, it is possible to manufacture 3D-net-shaped components with high tolerances, property consistency and efficient material utilization in large volume production [4, 5, 13].

3.2. Insulating Coating

The insulating coating that separates the individual iron powder particles in an SMC product is the paramount feature of this technology. Its thickness, coverage and endurance under the different processing operations are key aspects to the properties of a magnetic part. The insulating coating can serve dual purpose in a SMC component, that of increasing its bulk electrical resistivity and/or acting as a binder substance to improve its mechanical behavior. In general these coatings can be divided into two large families, namely organic and inorganic [4]. Most common methods for applying such surface layers on powdered materials are either immersion baths, sol-gel methods or through oxidation after annealing in the case of inorganic

coatings, while dissolving, mixing and drying, or polymerization on the powder's surface are the most preferred routes for organic coatings [6-8, 22-25].

The latter have been used extensively in powdered cores and can be divided into thermosetting and thermoplastic categories [4]. They are preferred due to the fact that they can act as binder medium and introduce good physical strength to a part, though they cannot be used in large volumes due to the reduction in permeability that they impose. A significant drawback for the organic coating usage is their thermal stability, especially for thermosetting resins, that does not allow an SMC part to be adequately stress relived at sufficient high enough temperatures for hysteresis losses reduction [23]. On the other hand, thermoplastic resins offer improved stability but have poorer coverage over the surface of the powder particles due to the difficulties in handling and processing.

The most common type of inorganic coatings used in the SMC technology are the phosphates (Zn/Fe/Mn), followed by oxides and sulfates [4]. Phosphatizing is a well establish metal conversion method and it has been used extensively in the steel industry [26]. Their robust application methods for large scale volume productions render them ideal for industrial usage. Phosphate based coatings possess an attractive combination of properties by providing good electrical insulation, anti-corrosive properties, thermal stability and can be functionalized and upgraded to more complex and improved structures [7, 8, 24, 25, 27].

3.3. Processing of SMC materials

An SMC part has to go through different processing steps in a production line in order to acquire its desired final form and properties. It should be understood that the combination of the base material choice and that of the processing parameters provides with a range of properties that can be tailored made for a desired application. It is obvious that these two are linked and the behavior and properties of the selected materials under the different processing steps will dictate the limits of the technique.

The manufacturing procedure of an SMC part via conventional PM production techniques starts with the base material selection. In most cases pure iron or a low alloyed iron-based powders containing Si, Ni, Al or Co and of various particle size distributions, typically produced by traditional water atomization techniques, are used [4, 5]. These grades are subsequently coated with the insulating surface layer, mixed with a lubricant and/or binder, compressed under uniaxial high pressures (up to 800 MPa) at net-shaped bodies and then subjected to post heat-treatment process, typically below 700°C [4].

The importance of the powder particle size, insulating coating and binder substance to the properties of an SMC part were mentioned earlier. The effect of lubricant is also important for the performance of a finished SMC component since it reduces inter-particles and particle to die wall frictions during compaction process, which can be proven detrimental to the coating's quality. The downside though of lubricant usage can be that the by-products produced during its degradation during the burn-off stage in the post heat-treatment process,

could also affect the nature of the coating by creating locally strong reducing atmospheres [9]. Moreover, an increased volume of the lubricant in a part has an inverse effect to its permeability and maximum flux density [11].

Under compaction process the SMC products are brought close to their final shape in as much less steps as possible, while at the same time higher density values are targeted which are essential for acquiring higher induction values. The process though introduces residual stresses to their bulk as well as high probability of damaging the insulating layer. These effects reduce the core losses of the component substantially by increasing the hysteresis and eddy current losses respectively [4, 11]. Different compaction techniques can be applied in order to get optimal results. These include warm compaction (where both the powder and the tool are heated), room temperature compaction, controlled die temperature compaction (where only the tool is heated up), two step compaction and high velocity compaction [4, 28].

To minimize the effect of the cold work imposed on an SMC part during its compaction, and subsequently to improve its properties, a post heat-treatment is required. Additionally, this step is required for the curing purposes when a binder is added, usually at lower temperatures [23]. The stress relief is a time-temperature related phenomenon and in principle, higher temperature regimes or longer dwelling times are needed for better tuning a component's properties. The time-temperature recipe though for a post heat-treatment step, as well as under which type of atmosphere this should take place, are largely dependent on the viability of the insulating layer during its process [9, 28]. It is thus crucial in the SMC technology that no sintering and no reduction of the coating should take place, since that would mean that its integrity been compromised and higher eddy current losses will achieved.

4. Materials and experimental details

For the purpose of materials characterization and modeling development a combination of complementary spectroscopic and microscopic analytical techniques were used. A detailed description of the materials under question along with experimental details related to the implementation of these techniques for such purposes is presented in the current section. The schema provided below in Figure 5 outlines the experimental procedure followed in this thesis and the materials used in every step.
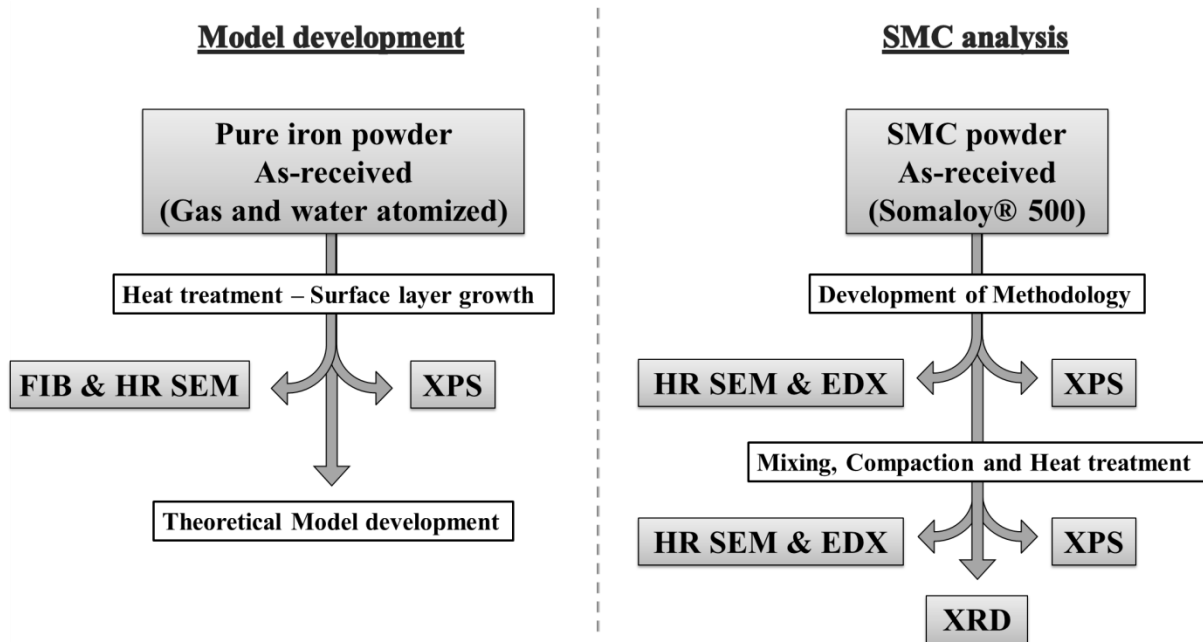
Figure 5: Schema of experimental investigations.

In this study two lines of experiments have been designed in order to reach its goals. In one of these (depicted to the left hand side of Figure 5), pure iron powder grades were investigated in Paper I as a base material for the development of the theoretical model for surface products thickness determination using HR SEM, FIB and XPS techniques. In the other (depicted to the right hand side of Figure 5), SMC as-received powder and finished components were analyzed in Papers II and III using HR SEM, EDX and XPS techniques for material characterization as well as process modeling and optimization purposes.

4.1. Materials

4.1.1. Pure iron powder

Pure iron powder produced by water atomization by Höganäs AB, Sweden, along with gas atomized iron powder of the same composition from a pilot atomizer were used for the experimental needs of the theoretical model development in Paper I. These grades have been

characterized elsewhere [29] based on their morphology, surface characteristics and chemistry. The water atomized powder exhibits a characteristic irregular shape as opposed to the spherical one of the gas atomized, while in both cases it was established that the surface was covered by a nano-sized homogeneous iron oxide layer. In the present work, both grades have been subject to further oxidation by heat treatment in air at 300°C prior to their analysis in order to grow sufficient thick surface oxide extended above the $3\lambda^{ox}$ limit (where λ^{ox} is the electron mean free path in the oxide layer) needed to implement the depth profiling technique in the XPS and also beyond the resolution limit of the HR SEM technique. In addition, both kinds of powder have been sieved down into a particle size fraction of 53-28 μm for minimizing any shading effects imposed by the sample roughness during the XPS investigations. The same powder fraction was also examined with focused ion beam (FIB) and high resolution scanning electron microscopy (HR SEM) for consistency purposes.

4.1.2. Somaloy® 500 material

The available commercial SMC powder grade Somaloy® 500 produced by Höganäs AB, Sweden, was used as a reference material. It consists of high purity water atomized iron powder, less than 150 μm in size, as a core structure coated individually with an ultra-thin inorganic electrically insulating surface layer under a patented process [22]. The powder was analyzed both in as-received form and in finished SMC components of toroidal shape, having 5x5 mm cross section and outer/internal diameter dimensions of 55mm/45mm respectively. The production of these parts for the current work included mixing of the SMC powder with 0.5 wt% of the commercial organic lubricant Kenolube™, compaction under conventional uniaxial die pressing at 800 MPa and heat treatment at 400, 500 and 600°C in air for 30 min, including de-lubrication and stress relief steps.

4.2. Analytical techniques

4.2.1. X-ray Photoelectron Spectroscopy

X-ray Photoelectron Spectroscopy (XPS) is a surface sensitive analytical technique that provides chemical compositional and chemical state information of the investigated material from a very small analysis depth of the order of few nanometers into the surface [30, 31]. Combined with ion etching technique it is possible to achieve depth profiling of the sample of interest. These attributes of XPS as well as its sensitivity to chemical environment changes (chemical peak shifts) and wide range of type of materials that can be examined makes it very appealing for surface and interface analysis in material science [32].

This technique has been used extensively for analysis of flat surfaces [31, 32] with an enormous amount of experimental methods and modeling efforts now available to the researcher. On the contrary, it has not been so popular for surfaces of specific geometry and roughness due to the anticipated shading effects from such samples and the subsequent uncertainties that these bring to the results. Previously, a theoretical model for analyzing

spherical particles using depth profiling technique combined with XPS was developed and experimentally tested by Nyborg et al. [33]. In their study, the effect of the surface geometry of the sample on the photoelectron intensity, X-ray flux and ion sputter rate was formulated for a specific experimental arrangement. By doing so, it was possible to evaluate the thickness of a homogeneous surface layer on a powder sample with a core-shell structure using depth profiling and by taking into account the normalized intensity of the substrate material at a certain relative metallic intensity fraction, defined by the relationship of the thickness of the layer over its attenuation length.

In this thesis, the XPS technique has been further implemented for developing the theoretical model and also to investigate the surface chemistry of the SMC powder in as-received state and finished components. In all cases a PHI 5500 (PERKIN ELMER, Eden Prairie, Minnesota, USA) instrument was used for analysis, equipped with a monochromatic Al K_α (1486.6 eV) X-ray source under ultra-high vacuum (UHV) conditions (1.3×10^{-12} bar). In the current experimental setup both the X-ray source and spectrometer axis formed a 45° angle with respect to the sample surface normal direction , as well as to the normal of the sample surface, while the ion gun was positioned at 50.5° from the sample surface. A schematic representation of this arrangement can be seen in Figure 6.
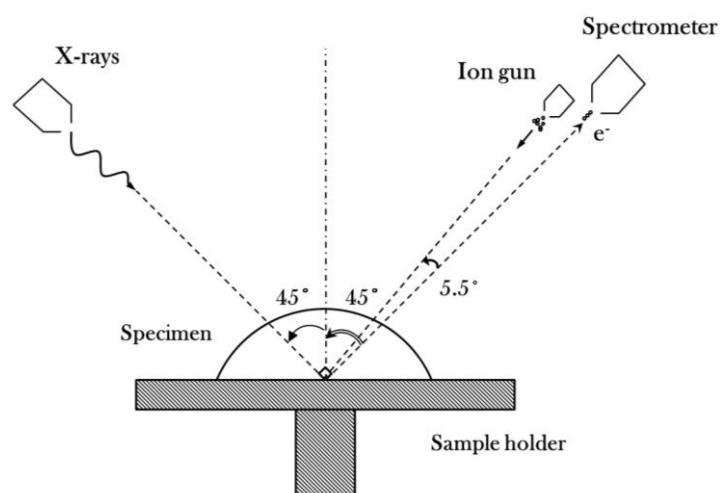
Figure 6: Experimental arrangement for XPS in current thesis.

Prior to the analysis, instrument calibration was performed using pure elemental standards (Au $4f_{7/2}$:84.00 eV, Ag $3d_{5/2}$:368.3 eV, Cu $2p_{3/2}$:932.7 eV). Additionally, ion sputtering rate calibration was carried out on flat oxidized tantalum foils (Ta_2O_5) of known thickness (100nm) yielding an etch rate of 21.6 Å min^{-1} over a rectangular area of $3 \times 4 mm^2$ at 3 kV or 50 Å min^{-1} over the same area at 4 kV ionization voltage. For all high resolution (HR) spectrum analyses, 23.5 eV pass energy and 0.1 eV/step were used while for all survey scans 93.9 eV and 0.4 eV/step respectively. The analyzing area was approximated at 0.8mm in diameter in all cases, which means that more than 100 powder particles being analyzed at the same time.

The heat-treated SMC components where fractured prior to their analysis and both outer and center regions of their cross sections were examined. The analyzed powder samples where loosely mounted on double adhesive conductive carbon tape in order to prevent any further deformation of the particles and ensure the integrity of the surface layers. The detected carbon signal was used as a reference value (C1s: 285 eV) for charge compensation purposes. Due to the high purity of the analyzed materials its presence was attributed to the existence of adventitious hydrocarbons on the samples surface, both for components and as-received powder. Charge compensation was performed in all cases using software correction and a low energy electron charge neutralizer flood gun. In later sputtering depths, where needed, the signal of the metallic iron was also used as a reference for charge peak shifting correction. The analysis and curve fitting of the collected spectra was performed with PHI Multipack software and for this an asymmetric Gaussian-Lorentzian line shape was preferred combined with Shirley background subtraction.

4.2.2. High Resolution Electron Microscopy

For the needs of surface morphology characterization of both powder samples and components, high resolution scanning electron microscopy (HR SEM) was implemented using a LEO Gemini 1550 (CARL ZEISS - LEO electron microscopy, GmbH, Germany) electron microscope equipped with a field emission gun. An in-lens secondary electron detector built in the electron column of the microscope was preferred for such type of analysis due to its high sensitivity at close working distances and low acceleration voltages, providing superior topographic and material work function related information with high lateral resolution. Energy dispersive X-ray spectroscopy (EDX) was also utilized as means of complementary chemical microanalysis in Papers II and III with an INCAEnergy system, though due to the inherent surface roughness of all samples the results were only evaluated qualitatively. Calibration for the microanalysis was conducted using elemental standards of cobalt for 20, 15 and 10 kV and silicon for 5kV. All powder samples were soft pressed into aluminum plates for HR SEM and EDX analysis while no special preparation was needed for the fractured surfaces of the components.

4.2.3. Focused Ion Beam

The focus ion beam (FIB) technique in combination with HR SEM were used in Paper I in order to determine the homogeneity and thickness of the surface layers from both gas and water atomized powder grades. The synergy of these techniques provides the user with the opportunity of performing in-depth analysis on sub-surfaces from exposed cross sectional regions created through a series of cutting and imaging of the material. This is achieved by having a dual beam system focused on the sample, consisting of an ion beam for sputtering and electron beam for imaging purposes. In this thesis a FEI Versa 3D DualBeam FIB–SEM station was used, equipped with a field emission gun (FEG) source and gallium high-current liquid metal ion source. Prior to the sputtering operations the samples where first gold coated before they were introduced to the station with an Edwards Sputter coater S150B and

subsequently a platinum layer of 2μm thickness was deposited on the site of interest *in situ* with an Omniprobe micromanipulator needle in order to protect the surface layer and achieve a sharp interface. The ion sputtering was carried out with gallium ions of 2 to 30 keV energy and 27 to 65000 pA beam current until the desired cross sectional surface quality was acquired. The samples were prepared by soft pressing the powder grades into aluminum plates similarly to the HR SEM analysis.

4.2.4. X-ray Diffraction

In the present work, the X-ray diffraction was used for phase identification analysis of the exterior surface of SMC heat treated components at different temperature regimes. The experimental measurements were carried out using a Bruker D8 ADVANCE diffractometer equipped with a Cr-Kα source under grazing angle mode at an incident angle of 3 degrees over a range of $40° < 2θ < 140°$ with $0.05°$ $2θ$/step and 5 sec/step. The penetration depths of the X-rays for the compounds of interest were calculated with the AbsorbDX V.1.1.4 software.

5. Results and summary of appended papers

In this section of the thesis the results and a summary of the appended papers are given, along with key discussion points and some complementary material to better illustrate all of the above where needed. In Paper I the further development of the existing theoretical model [33] for estimating the thickness of homogeneous surface layers on substrates of spherical shape using depth profiling technique with XPS was presented. The model's formulation was introduced and its validity was experimentally assessed using XPS on pure iron powder grades of regular and irregular morphologies. Additional analytical techniques such as FIB – HR SEM were also implemented for confirmation of the results. In Papers II and III the SMC as-received powder and finished components, respectively, were analyzed. In the first case a methodology was developed based on XPS, HR SEM and EDX techniques for chemical, topological/morphological and depth profiling analysis of such type of insulating layers. Different sample preparation and charge compensation methods were tested and optimum conditions for imaging and chemical analysis were established. In the second case, SMC finished components were investigated using HR SEM, EDX, XPS and XRD techniques. The effect of the temperature to the different regions of a part and to the thermal stability of the surface insulating coating was evaluated.

5.1. Theoretical model development for layer thickness determination on powder

The experimental arrangement influences the result of an XPS depth profiling analysis when this regards materials of specific geometry and roughness. As opposed to flat surfaces, inherent shading effects can be introduced and influence the result due to their irregular morphologies. Additionally, the X-ray flux, photoelectron intensity and ion sputter rate are not constant locally when probing such type of surface irregularities but exhibit an angle dependency over the whole analyzed surface area. In particular, this type of dependency of the ion sputtering rate results in non-homogeneous material removal over the probed area and the positioning of the ion gun in space in respect to the spectrometer and to the X-ray source dictates the amount of residual layer that will be analyzed. In Figure 7 an attempt to illustrate this effect is shown for the case of a spherical core-shell structure (the dashed interior sphere represents the core while the yellow colored exterior sphere the homogeneous surface layer) examined with an arbitrary experimental setup. There, the residual surface layer (colored in orange) that will be measured from the analyzed area (dark shaded region) depends on the position of the ion gun in the three dimensional space.
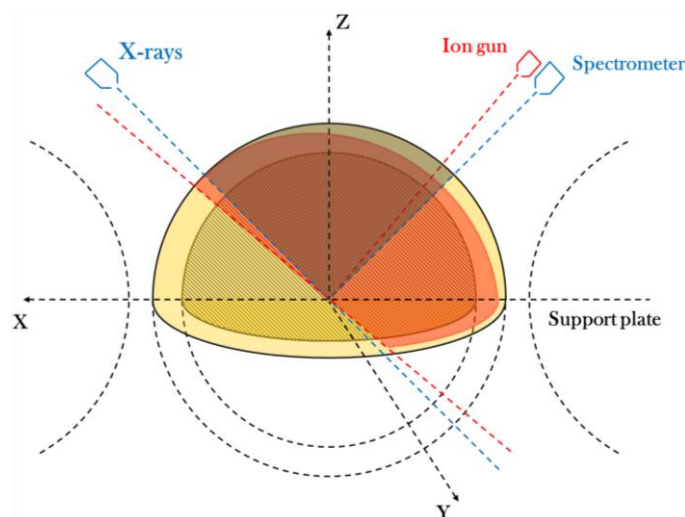
Figure 7: A schematic illustration of the effect of the incident ion beam angle on the analysis of a spherical surface with XPS.

Hence, the purpose of the development of the theoretical model in Paper I was to introduce geometrical freedom in terms of experimental setup and to create a versatile tool that could match the specifications of any equipment used for such type of analyses. In order to do so, each analyzed particle is considered as a hemisphere which is unshaded from its neighbors having a homogeneous surface layer larger than $3\lambda^{ox}$ while the ion gun, the X-ray source and the spectrometer axes are defined in space by different sets of spherical coordinates.
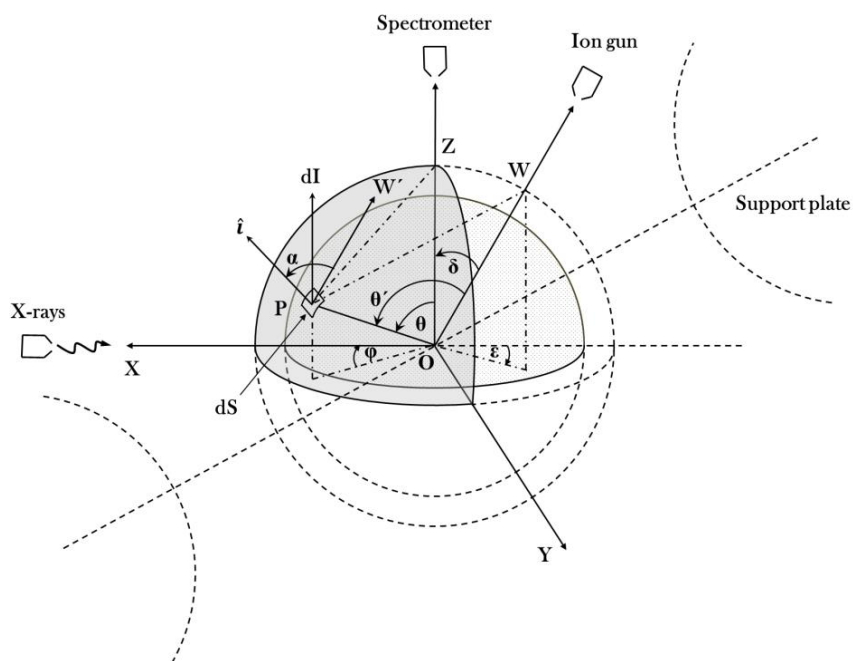
Figure 8: A schematic representation of a spherical core-shell structure analyzed by an arbitrary experimental arrangement in XPS (Image taken from Paper I).

In Figure 8, the spherical coordinates of a random point **P** on the analyzed area of a particle surface (shaded area) are depicted as well as the relationships between the X-ray source, the spectrometer and the ion gun. All these considerations where taken into account in Paper I and a relationship that defined the recorded intensity at each point of interest was formulated according to equation (1):

$$I = iR^2 \int_{\theta_1}^{\theta_2} \int_{\varphi_1}^{\varphi_2} F \cos\theta \sin\theta |\cos(\zeta - \theta)| \cos\varphi \, d\theta d\varphi \quad (1)$$

The latter, along with a profile for the angle effect on the sputtering rate, were implemented in order to calculate the residual surface layer (t^{ox}) at every point **P** of the analyzed area. These calculations were carried out utilizing an iterative process in a custom developed computer software for which only the experimental and material dependent parameters mentioned above are needed (Figure 9).
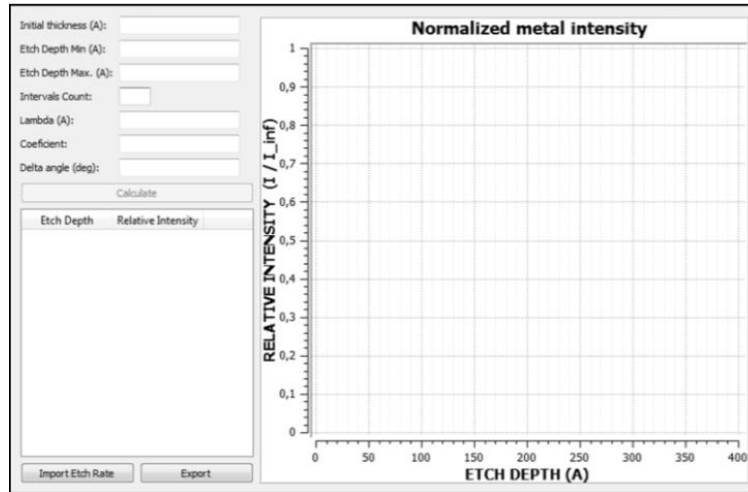
Figure 9: User interface of a developed computer software for calculating the relative substrate intensity *versus* etch depth.

In this manner, characteristic ´s´ type curves of the relative intensity of the substrate in respect to the etch depth are acquired for surface layers of known thicknesses and attenuation lengths (λ^{ox}) as shown in Figure 10 for two different materials. These results show that there is a strong dependency of the relative intensity value with increasing λ^{ox} and with increasing layer thickness, where in the first case it increases while in the second it decreases.
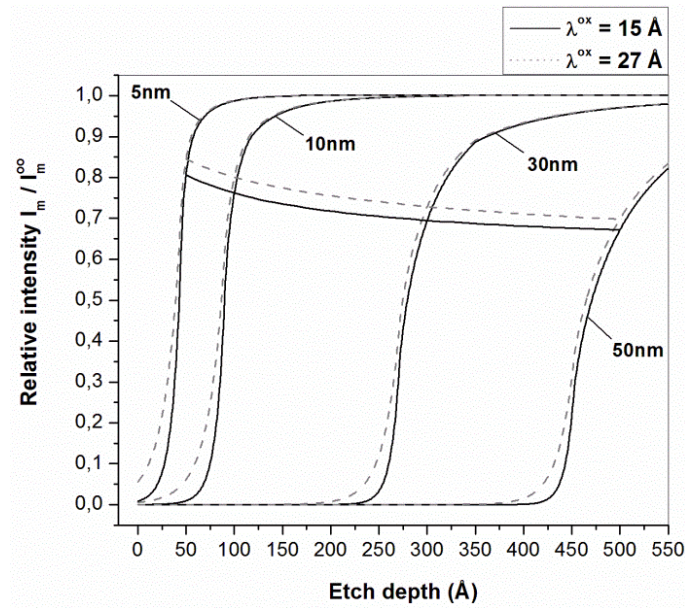
Figure 10: Relative substrate intensities *versus* etch depth calculated for two different λ^{ox} values and different thicknesses of surface layers (Image taken from Paper I).

The theoretical model was experimentally tested on pure iron powder of irregular and spherical shapes, as mentioned earlier in the experimental section, in order to evaluate the effect of the surface morphology and roughness on the thickness estimation. Additional to their XPS analysis both grades where cross sectioned with FIB and subsequently analyzed with HR SEM to determine the thickness variation and homogeneity of the surface layer as shown in Figure 11.

Subsequent XPS depth profile analysis was performed for both grades and the values acquired from the experimental profiles for the relative metallic intensity values at the interface, as it was defined earlier from the FIB – HR SEM analysis, were compared with the ones provided from the model. This comparison showed a minor deviation, around 3%, for both grades that could be attributed to the surface microtopography, which introduces a certain degree of localized shading effects as well as the small variation in the layer thickness estimation by HR SEM.

Oxide thickness estimation (FIB - HR SEM)	Water atomized powder	Gas atomized powder
	65.5 ± 14.9 nm	38.14 ± 7 nm
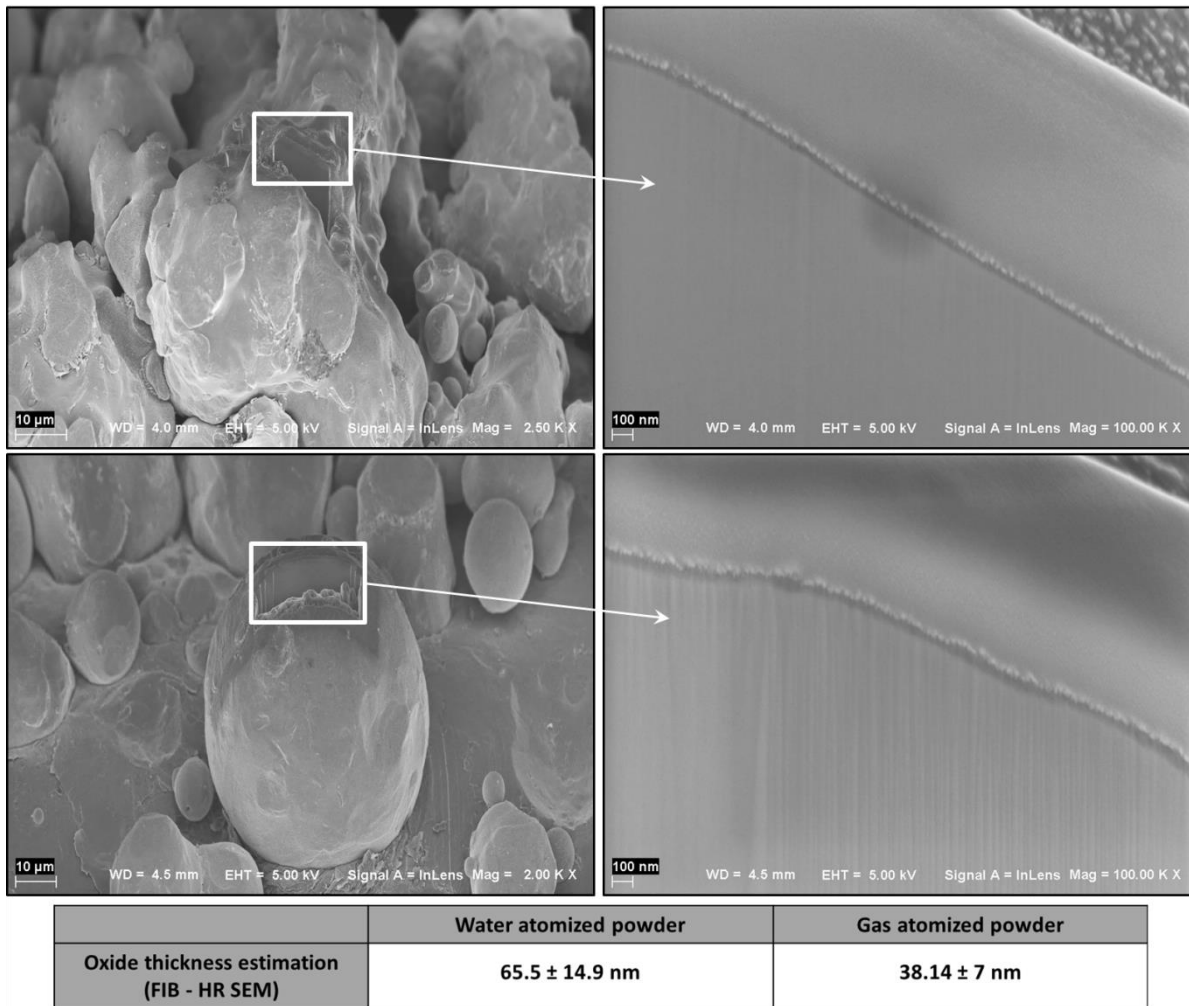
Figure 11: Analyzed cross sections of powder particles from both grades with FIB – HR SEM

5.2. Characterization of SMC powder

To characterize the initial state/composition of the insulating coating of the SMC material, a robust methodology needed to be established based on analytical techniques. Initially, the as-received SMC powder was investigated with HR SEM and EDX with different experimental settings in order to determine the optimal conditions for evaluating the coatings morphology, cohesion and coverage of the surface. A range of acceleration voltages from 5 to 20 kV and aperture sizes of 30μm or less were tested in Paper II as to efficiently enough reduce the beam spot size and interaction volume. The results are shown in Figure 12 where it can be observed that with increasing acceleration voltage, due to the higher energy of the secondary electrons emitted, the information acquired from the very top surface is significantly less and the features of the coating are no longer visible. Additionally, regarding the chemical microanalysis, it is shown that at lower acceleration voltage it is possible to still excite all the elements present at the surface layer and better distinguish between the core material and the coating regions. By implementing the above optimum conditions, HR SEM and EDX analysis revealed the good coverage of the insulating layer over the particles surface, its homogeneity

in terms of surface feature characteristics and the rare presence of delaminated regions close to particle irregularities.
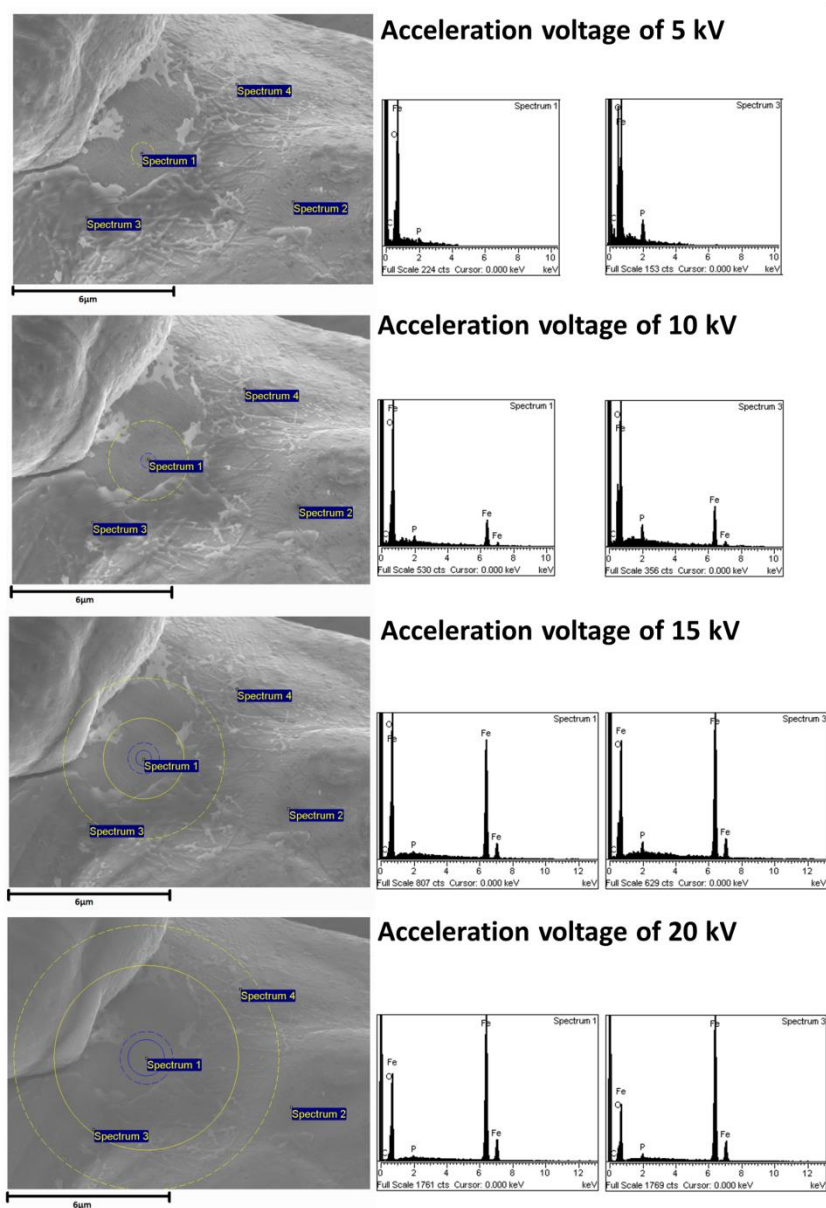
Figure 12: Qualitative EDX point analysis of as-received SMC power under different acceleration voltages (5, 10, 15 and 20 kV) (Image taken from Paper II).

For the XPS analysis of the as-received powder two sample preparation methods were tested as to determine the most suitable for tackling charging effect during measurements and for ensuring the integrity of the coating. In one case the SMC grade was softly pressed into aluminum plates while in the other it was loosely spread over adhesive conductive carbon tape. For both methods charge compensation using an electron flood gun and software correction were implemented. The results revealed the presence of the same elements in the surface for both cases (oxygen, phosphorus, iron, carbon and traces of nitrogen) with the exception of a slightly higher carbon signal for the powder mounted on the carbon tape. It was thus preferred to apply the latter method as the preservation of the insulating coating state was

much more ensured as no mechanical force was applied on the particles during specimen preparation. The chemical compositional analysis of the powder with the HR scans showed that the surface layer consists of ferric and ferrous iron phosphate compounds. The stability of the phosphorus signal to the sputtering operations indicated its homogeneous nature throughout coating's depth. Moreover, the analysis of the oxygen signal after successive ion sputtering steps exposed a transition from the PO_4^{3-} group to the O^{2-} compound, which accounted to the oxide Fe_2O_3 close to the interface between the matrix and the surface layer. The implementation of the model for layer thickness determination to the as-received powder was also performed based on the XPS depth profiling analysis and the thickness evaluation of the surface layer was estimated based on the normalized signals of its constituent elements (Figure 13). From the latter became apparent that the coating was in the nano-meter scale and based on the phosphorus signal, which can be solely assigned to the presence of the insulating coating, its thickness could be estimated at about 23 nm.
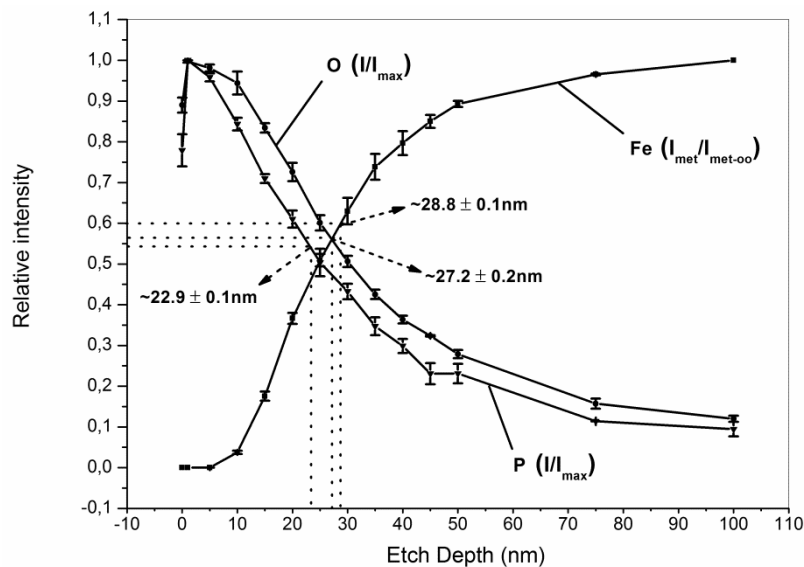
Figure 13: Normalized intensities of Fe metal, oxygen, and phosphorous *versus* etch depth for SCM as-received powder (Image taken from Paper II).

5.3. Investigation of finished SMC components

In order to investigate the temperature effect on the finished SMC components, three different regimes were chosen namely at 400, 500 and 600°C based on previous investigations on the magnetic and mechanical properties of these type of materials. Initial optical stereoscopic micrographs of the fracture surfaces revealed an evident discoloration throughout the cross section of the sample treated at 400°C as compared to the rest, implying a difference in the effect of the post heat-treatment between different temperatures and along the length of a single sample. Subsequent HR SEM analyses of both outer and interior regions of the fractured surfaces of all heat-treated components showed a difference in the morphology, homogeneity, coverage and cohesion of the developed surface layer. In the outer regions of all

samples a complex multi-layered structure was observed comprised of a thick scale that extended between the compressed powder particles as shown in Figure 14.
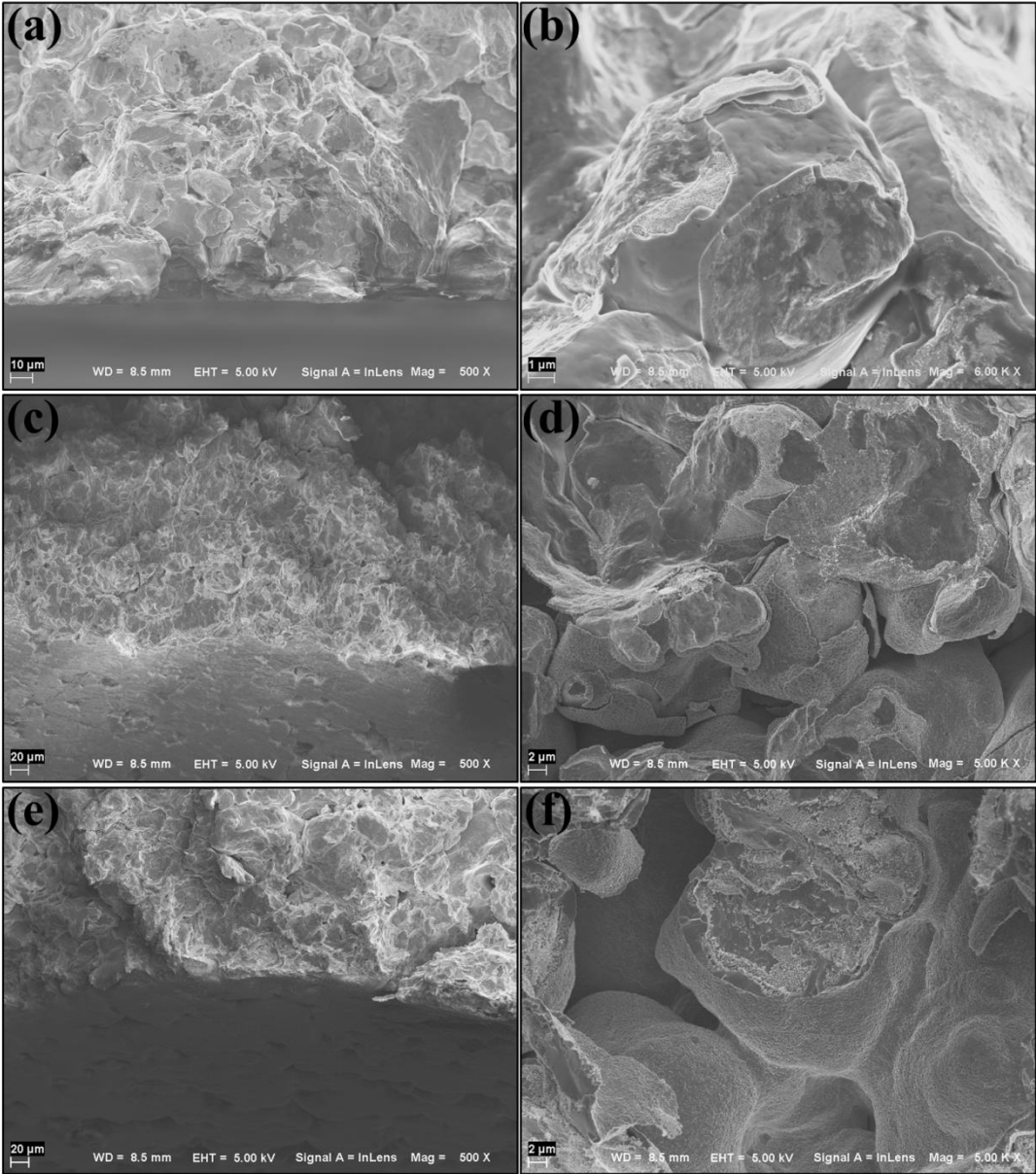
Figure 14: HR SEM micrographs of the outer regions of the SMC heat-treated components at 400°C (a-b), 500°C (c-d) and 600°C (e-f).

The analysis of the exterior surface of the components with XRD under grazing angle showed that the scale was consisting of iron oxides, mainly magnetite and hematite. It was also noted that the thickness of it increases with the temperature. These results were also in accordance with the qualitative point analysis performed with EDX on the scale for all temperatures where iron and oxygen were the main constituent elements. On the contrary, the surface layer present in the interior region of the parts appeared to be very thin as compared to the outer region comprising of two distinct areas of different contrast. These are easier to observe at higher magnifications, Figure 15 (b, d and f), where the open areas have lighter contrast while

the particle to particle connections appear darker and with a 'net' type of structure. In particular, at 400°C these areas are more pronounced and the chemical microanalysis with EDX showed that they are more enriched with carbon and zinc as compared to the matrix, which is an indication of the presence of residual compounds from the incomplete de-lubrication of the parts for those temperature regimes.
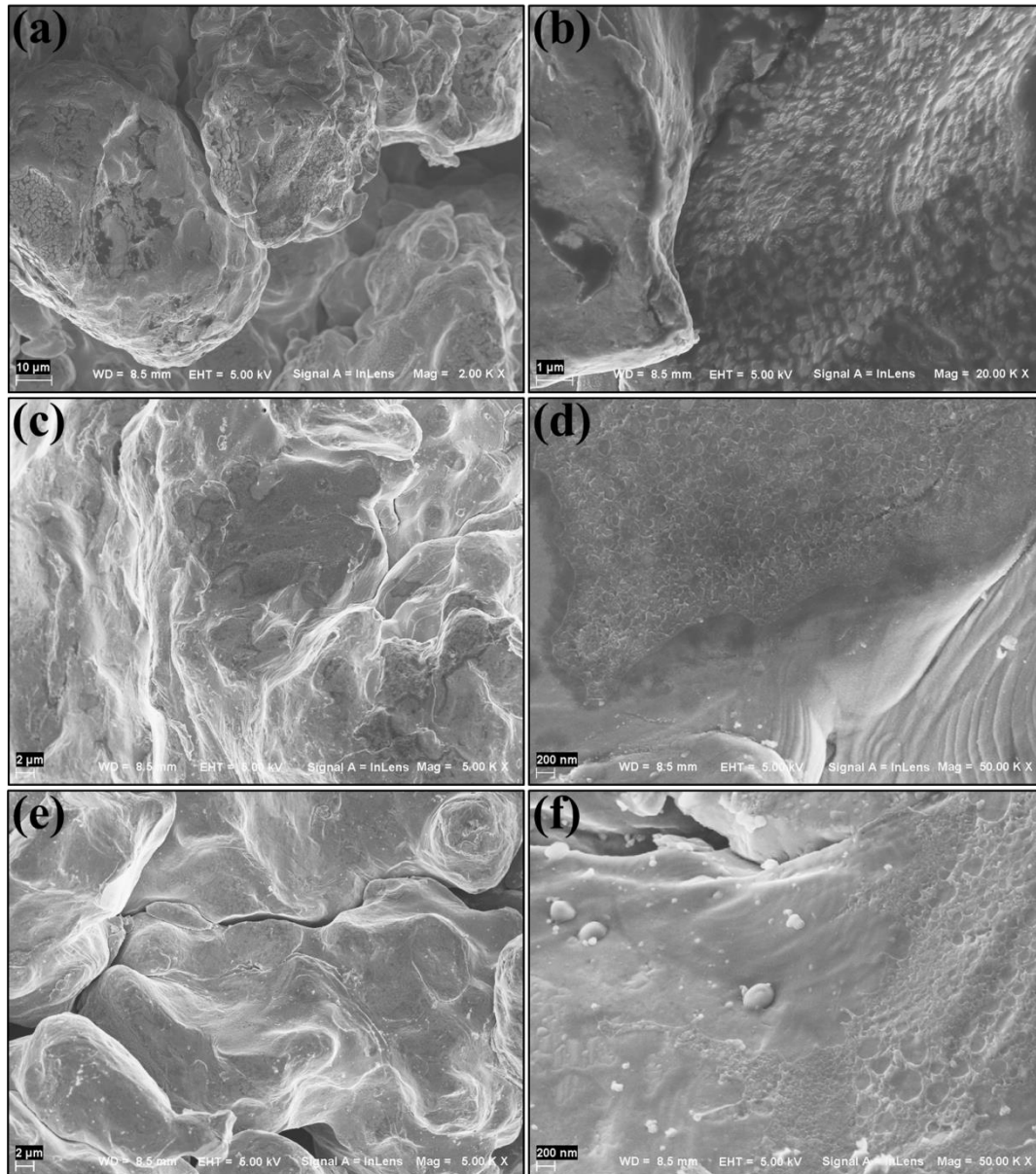
Figure 15: HR SEM micrographs of the interior regions of the SMC heat-treated components at 400°C (a-b), 500°C (c-d) and 600°C (e-f).

To further investigate the effect of the temperature on the surface coating, XPS analyses were performed for both the interior and exterior regions of all samples. The apparent atomic concentration profiles showed that for the outer regions a higher amount of carbon is always detectable as compared to the interior, stating that the residuals of the organic based lubricant containing heavy hydrocarbons are decomposing on the outermost surface of the component.

Moreover, the carbon content in the fracture surface of the interior region of the sample treated at 400°C was also higher as compared to the rest samples, showing that the incomplete de-lubrication is even more evident at that regime. The HR XPS spectrum analysis of all surface layers, for both regions, indicated that they consist mainly of a mixture of iron oxides and iron phosphates of both divalent and trivalent forms. In particular, the oxygen signal analysis at 400°C showed the oxidation was more pronounced in both regions compared to the rest samples. This result coupled well with those from the imaging and XRD analysis and it was concluded that the insufficient closure of the external porosity from the oxide scale growth at low temperatures lead to the extended oxidation of the component throughout its cross section.

By further analyzing the HR XPS spectra, a small secondary peak after ion sputtering was observed for all temperatures in the phosphorus signal. Its presence was not attributed to the PO_4^{3-} species but to transitional metal phosphides. Theoretical thermodynamic calculations performed in Paper III supported their existence close to the interfacial region between the surface layer and the matrix due to the abundance of iron and the low oxygen partial pressure that exist in a PM compact. In addition, in Figure 16 the ratio between the phosphorus and iron content is depicted for the heat-treated components in Paper III along with the same type of analysis for the as-received powder from Paper II. It can be observed that the 500°C sample has the highest measured value for the P/Fe concentration ratio, while 600°C and 400°C follow.
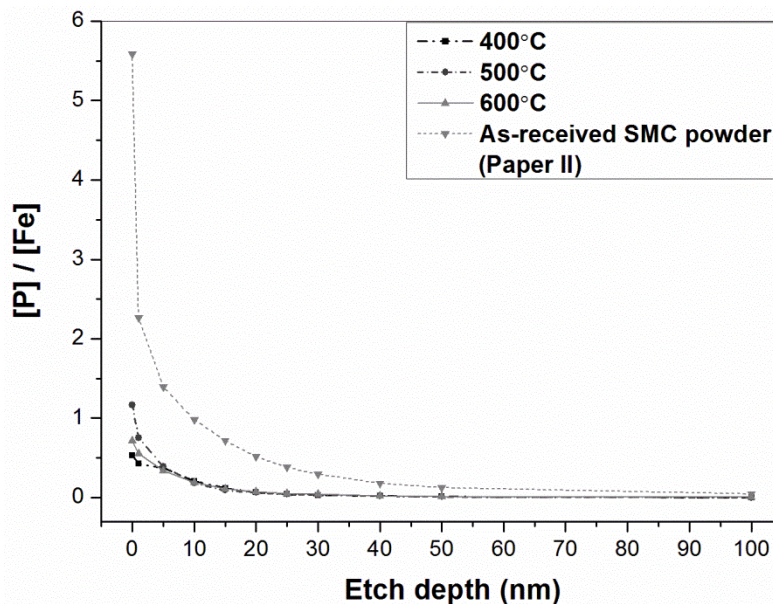
Figure 16: Ratio of phosphorus and iron content *versus* etch depth for all heat-treated samples from Paper II (interior regions) and as-received powder from Paper III.

Finally, the theoretical model was qualitatively implemented to the fracture surfaces under the considerations that the degree of surface roughness was acceptable and reproducible based on the small standard deviation values from the repeated measurements (Figure 17). By doing so, the relative intensities of iron signal showed that the total surface layer at 400°C was thicker

while for the other two regimes the differences were too small and comparable to the standard deviation. The relative intensities of the phosphorus signal though showed that all temperature profiles are very close to each other, with the one at 400°C being the broadest followed by the 500°C and 600°C. By combining all this information from these profiles and the from the P/Fe concentration ratio analysis depicted in Figure 16 it may be plausible to assume that at 400°C the open porosity of the sample allows its further oxidation in its interior region and thus the presence of a thicker oxide layer. For the cases of 500°C and 600°C though the growth of the exterior scale prevents this mechanism to take place to a great extent. Still though, oxygen diffusion through the scale takes place in both of these cases and in particular at 600°C, where the kinetics are faster. A slight increase in the thickness of the surface layer is observed as compared to the one at 500°C, due to its further oxidation. The latter can also correlate to the HR XPS spectra analysis of the oxygen signal, where the O^{2-} shoulder is slightly broader for the fractured sample heated at 600°C.
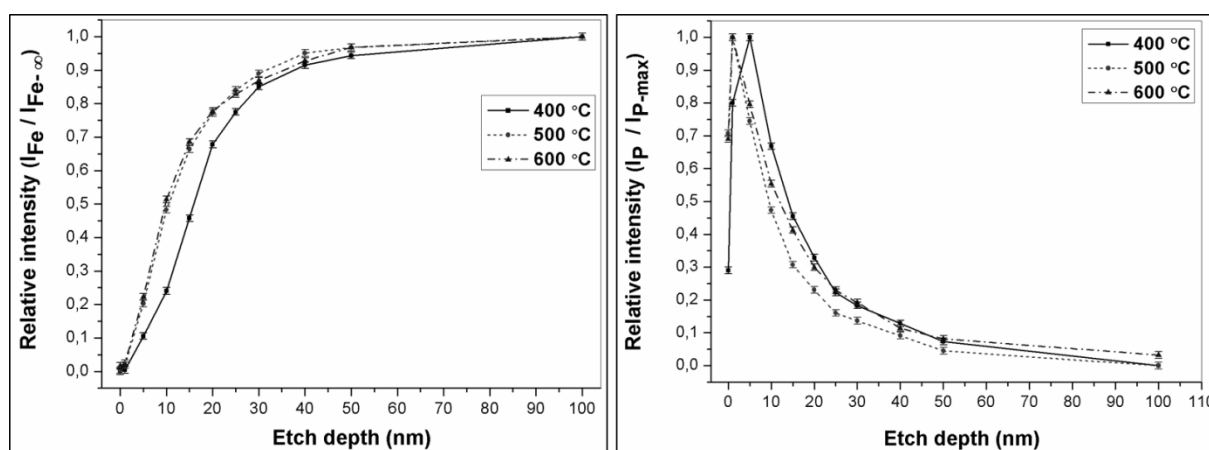
Figure 17: Normalized intensities of interior regions of SMC components heat treated at 400, 500 and 600 °C for Fe metallic (left) and phosphorus (right) signals vs etch depth. (Image taken from Paper III)

6. Conclusions

In the present study, the following concluding remarks can be highlighted:

Theoretical model for thickness evaluation of surface coatings on metal powder

- A theoretical model for estimating the thickness of surface layers on particles of spherical shape using XPS depth profiling technique without any geometrical constraints related to the experimental arrangement has been developed.
- The model was experimentally tested with XPS and validated using XPS and FIB - HR SEM analytical techniques and the deviation between theoretical and experimental values was of the order of 3%.
- It is possible to apply the model with good agreement for routine measurements on surfaces of specific geometry and roughness in the range of up to hundred micrometers.

Methodology development for surface analysis of SMC powder

- A methodology was developed for the evaluation of the composition, morphology and thickness of the insulating layer of SMC powder grades.
- Optimum conditions for HR SEM and EDX analysis were defined at 5kV acceleration voltage and low beam current using in-lens secondary electron detector.
- Adhesive carbon tape was evaluated as the optimal method for sample preparation for XPS analysis.
- Analysis reveals oxygen, iron, and phosphorous as the main constituents of the insulating coating.
- The surface coating was found to be stable under ion sputtering operations.
- Coating thickness evaluation based on the normalized intensities of the metallic iron, phosphorus and oxygen signals show that it ranges bellow 30nm.

Heat-treatment of SMC components

- The effect of temperature on the surface layer morphology, homogeneity, cohesion and composition was evaluated using XPS, HR SEM, EDX and XRD techniques for SMC finished components.
- For all temperatures two regions, an exterior and an interior, can be distinguished having significant differences in the degree of oxidation.
- For all temperatures the exterior region appears to be considerably oxidized and the presence of an iron oxide scale that increases in thickness with temperature was confirmed as the dominant surface constituent.
- Analysis of all interior regions revealed the presence of a blend of iron phosphates and iron oxides both in divalent and trivalent form.
- The presence of impurity oxide particulates and iron phosphide precipitates dispersed in the insulating surface layer were confirmed as a result of the post heat treatment.
- HR-SEM, EDX and XPS analyses showed the presence of higher amounts of lubricant residuals enriched in Zn due to the incomplete de-lubrication process for the interior region of the sample treated at 400°C.

- Qualitative implementation of a theoretical model for surface layer thickness determination based on XPS depth profiling showed for 400°C that the insulating layer is associated with a broader profile, i.e. more extended presence along the etch depth, which can be attributed to stronger presence of iron oxides.

7. Suggestions for future work

7.1. Theoretical model development

For further experimental validation of the theoretical model, point analysis with the auger electron spectroscopy (AES), as well as transmission electron microscopy (TEM) and electron backscatter diffraction (EBSD) on powder particle cross sections can be utilized in order to fully characterize the materials under investigation and so to eliminate any ambiguities in regard to their thickness evaluation.

Furthermore, the theoretical model is possible to be extended to surfaces of higher roughness, e.g. fracture surfaces, and acquire quantitative results. In order to do so, it must be combined with methods or techniques that provide quantification of roughness on a micro level, e.g. MeX for SEM, and evaluated experimentally on fully characterized materials with complementary analytical techniques.

7.2. SMC analysis

Complementary results to the ones acquired from the analysis of the SMC heat-treated components can yield heat-treatments on the as-received powder alone. By doing so, the effect the lubricant present can be eliminated and additionally the theoretical model could provide quantification of the coating's thickness determination.

Moreover, additional analysis by AES on the fractured surfaces could reveal more information on the nature of the phosphide phases present as well as information on the composition and thickness of the coating between particle to particle contacts and open (pore surface) areas.

8. Acknowledgments

9. References

[1] Energy efficiency and specific CO2 emissions, Retrieved March 27, 2014, *http://www.eea.europa.eu/data-and-maps/indicators/energy-efficiency-and-specific-co2-emissions*

[2] O. Gutfleisch, M.A. Willard, E. Bruck, C.H. Chen, S.G. Sankar, J.P. Liu, *Magnetic materials and devices for the 21st century: stronger, lighter, and more energy efficient*, Advanced materials, 23, 7, (2011) 821-842.

[3] W.T. McLyman, *Transformer and Inductor Design Handbook - Fourth Edition*, Taylor and Francis Group, LLC, (2011)

[4] H. Shokrollahi, K. Janghorban, *Soft magnetic composite materials (SMCs)*, Journal of Materials Processing Technology, Vol. 189, No. 1-3, (2007) 1-12.

[5] M. Persson, P. Jansson, A.G. Jack, B.C. Mecrow, *Soft Magnetic Composite Materials - Use for Electrical Machines*, IEEE Conference Publication, No. 412, (1995), 242-246.

[6] H. Bruncková, M. Kabátová, E. Dudrová, *The effect of iron phosphate, alumina and silica coatings on the morphology of carbonyl iron particles*, Surface and Interface Analysis, Vol. 42, No. 1, (2010) 13-20.

[7] A.H. Taghvaei, H. Shokrollahi, K. Janghorban, H. Abiri, *Eddy current and total power loss separation in the iron–phosphate–polyepoxy soft magnetic composites*, Materials & Design, Vol. 30, No. 10, (2009) 3989-3995.

[8] S. Wu, A. Sun, W. Xu, Q. Zhang, F. Zhai, P. Logan, A.A. Volinsky, *Iron-based soft magnetic composites with Mn–Zn ferrite nanoparticles coating obtained by sol–gel method*, Journal of Magnetism and Magnetic Materials, Vol. 324, No. 22, (2012) 3899-3905.

[9] P. Jansson, *Processing aspects of soft magnetic composites*, Proceedings of the Euro PM2000 Conference Soft Magnetic Materials Workshop, Munich, Germany, (2000), 9-14.

[10] B.D. Cullity, C.D. Graham, *Introduction to Magnetic Materials, Second Edition*, IEEE Press, (2009)

[11] H. Skarrie, *Design of Powder Core Inductors*, Lund University, Sweden, (2001).

[12] Y. Zhang, M.-C. Cheng, P. Pillay, *Magnetic Characteristics and Excess Eddy Current Losses*, Proccedings IEEE Industry Applications Society Annual Meeting, (2009), 1-5.

[13] L.O. Hultman, A.G. Jack, *Soft Magnetic Composites - Materials and Applications*, Electric Machines and Drives Conference, IEMDC'03, IEEE International, Vol. 1, (2003), 516-522.

[14] ARNOLD Magnetic Technologies, Soft Magnetics Applications Guide, Retrieved March 29, 2014, *http://www.arnoldmagnetics.com/Soft_Magnetics_Applications_Guide.aspx*

[15] Höganäs AB. Somaloy Technology, Applications, Retrieved March 29, 2014, *http://www.hoganas.com/en/Segments/Somaloy-Technology/Applications/*

[16] AMES, Soft Magnetic Parts, Retrieved March 29, 2014, *http://www.ames.es/products/1037-2/*

[17] K. Narasimhan, F. Hanejko, M.L. Marucci, *Soft magnetic material for A.C. applications*, Hoeganes Corporation, Available from http://www.yunamedia.com/GKNPLCHC.com/KyungHoeganae/TechPapersv2/201.pdf.

[18] O. Larsson, *Fe-based Amorphous Powder for Soft-Magnetic Composites*, Department of Materials Science and Engineering, Royal Institute of Technology, Stockholm, Sweden, Master Thesis, (2013).

[19] C. Suryanarayana, A. Inoue, *Iron-based bulk metallic glasses*, International Materials Reviews, Vol. 58, No. 3, (2013) 131-166.

[20] O. Andersson, P. Hofecker, *Advances in Soft Magnetic Composites – Materials and Applications*, International Conference on Powder Metallurgy & Particulate Materials, PowderMet 2009, Las Vegas, Nevada, 2, (2009). ISBN: 978-0-9819496-1-1

[21] GKN Sinter Metals - Soft Magnetic PM, *http://www.gkn.com/sintermetals/capabilities/soft-magnetic-pm/Pages/default.aspx*

[22] P. Jansson, *Phosphate coated iron powder and method for the manufacturing thereof*, No. US 6,348,265 B1, Feb. 19, (2002)

[23] I. Hemmati, H.R.M. Hosseini, S. Miraghaei, *Effect of processing parameters on electrical,mechanical and magnetic properties of iron-resin soft magnetic composite*, Powder Metallurgy, Vol. 50, (2007) 86-90.

[24] S. Rebeyrat, J.L. Grosseau-Poussard, J.F. Dinhut, P.O. Renault, *Oxidation of phosphated iron powders*, Thin Solid Films Vol. 379, No. 1-2, (2000) 139-146.

[25] A.H. Taghvaei, H. Shokrollahi, K. Janghorban, *Properties of iron-based soft magnetic composite with iron phosphate–silane insulation coating*, Journal of Alloys and Compounds, Vol. 481, No. 1-2, (2009) 681-686.

[26] K. Ogle, M. Wolpers, *Phosphate Conversion Coatings, Corrosion: Fundamentals, Testing, and Protection*, ASM Handbook, ASM International, Vol. 13A, (2003) 712-719.

[27] R. Balasubramaniam, *On the corrosion resistance of the Delhi iron pillar*, Corrosion Science, Vol. 42, (2000) 2103-2129.

[28] Y. Zhou, L. Hultman, L. Kjellen, *Production Aspects of SMC Components*, Powder Metallurgy World Congress & Exhibition, Vol. 4, (2004), 552-559.

[29] D. Nikas, *Characterization of electrically insulating coatings for soft magnetic composite materials by means of surface sensitive analytical techniques*, Materials and Manufacturing Department, Chalmers University of Technology, Gothenburg, Sweden, MSc Thesis, (2013).

[30] C.D. Wagner, W.M. Riggs, L.E. Davis, J.F. Moulder, G.E. Muilenberg, *Handbook of X-ray Photoelectron Spectroscopy*, Perkin-Elmer Corporations, Physical Electronics, Minesota, USA, (1979)

[31] J.F. Watts, J. Wolstenholme, *An introduction to Surface Analysis by XPS and AES*, John Wiley & Sons, Ltd, Chichester, UK, (2005) DOI:10.1002/0470867930

[32] D. Briggs, M.P. Seah, *Practical surface analysis: Auger and X-ray photoelectron spectroscopy*, Vol. 1, John Wiley and Sons Ltd, (1990)

[33] L. Nyborg, A. Nylund, I. Olefjord, *Thickness determination of oxide layers on spherically-shaped metal powders by ESCA*, Surface and Interface Analysis, Vol. 12, No. 1-12, (1988) 110-114.